Anti-Amyloid Activity of the C-Terminal Domain of proSP-C against Amyloid β-Peptide and Medin[†]

Charlotte Nerelius,[‡] Magnus Gustafsson,[‡] Kerstin Nordling,[‡] Annika Larsson,[§] and Jan Johansson*[,‡]

Department of Anatomy, Physiology and Biochemistry, Swedish University of Agricultural Sciences, The Biomedical Centre, 751 23 Uppsala, Sweden, and Department of Genetics and Pathology, Uppsala University, Rudbeck Laboratory, 751 85 Uppsala, Sweden

Received January 28, 2009; Revised Manuscript Received March 11, 2009

ABSTRACT: Amyloid fibrils are found in ~25 different diseases, including Alzheimer's disease. Lung surfactant protein C (SP-C) forms fibrils in association with pulmonary disease. It was recently found that the C-terminal domain of proSP-C (CTC), which is localized to the endoplasmic reticulum (ER) lumen, protects the transmembrane (TM) part of (pro)SP-C from aggregation into amyloid until it has a folded into an α-helix. CTC appears to have a more general anti-amyloid effect by also acting on TM regions of other proteins. Here we investigate interactions of CTC with the amyloid β-peptide (Aβ) associated with Alzheimer's disease and medin, a peptide that forms fibrils in the most common form of human amyloid. CTC prevents fibril formation in Aβ and medin and forms a complex with Aβ oligomers, as judged by size-exclusion chromatography and electrospray ionization mass spectrometry. These data suggest that CTC functions as a chaperone that acts preferentially against unfolded TM segments and structural motifs found during amyloid fibril formation, a mechanism that may be exploited in forming a basis for future anti-amyloid therapy.

A large number of diseases are caused by aberrant folding and aggregation of proteins, so-called misfolding diseases. A subset of these diseases, including for example Alzheimer's disease, Parkinson's disease, and prion diseases, is associated with a specific form of misfolding whereby native solubility and structure are lost and replaced with aggregation into highly insoluble amyloid fibrils with β-sheet structure (*1*). Amyloid fibrils are composed of β-strands running perpendicular to the axis of the fibril (*2*). The morphology of the fibrils as revealed by electron microscopy is very similar regardless of the polypeptides involved. This fact and the apparent lack of sequence similarity between the proteins that form fibrils suggest that virtually all proteins could adopt a fibrillar structure (*3*). However, only ~25 polypeptides are known to form fibrils in association with mammalian disease (*1*). Previously, it was believed that the mature fibrils as such are cytotoxic and thereby cause disease, but more and more evidence points to the toxic nature of smaller soluble intermediates formed in the earlier stages of amyloid fibril formation (*4, 5*).

Alzheimer's disease is a progressive neurodegenerative disorder characterized by the presence of extracellular amyloid deposits, so-called plaques, which contain the amyloid β-peptide (Aβ).[1] Aβ consists of 40−42 amino acids and is cleaved from the amyloid precursor protein (APP) by β- and γ-secretase (*6*). The released peptide, Aβ, contains a part of the transmembrane (TM) region of APP (Aβ residues 29−40/42) and includes a discordant helix, i.e., a helix composed of amino acids with a high propensity to form β-strands (*7*). Aβ is prone to misfold and aggregate when removed from its stabilizing membrane environment (*8*).

The process of Aβ amyloid fibril formation is far from being completely understood. So far, no structural information about Aβ oligomers, apart from the approximate number of constituent Aβ molecules, is available, making design of aggregation inhibitors a difficult task. One suggested strategy for preventing aggregation has been to utilize chaperones. Chaperones play an important role by aiding the correct folding of proteins in the complex intracellular milieu. A number of molecular chaperones, such as heat-shock proteins (Hsp), are known to be important in the folding process and have been extensively studied. Some of these chaperones are apparently able to interact with and have an impact on the amyloid fibril formation of certain polypeptides. Aggregation of $A\beta_{1-42}$ is inhibited by Hsp90 or the combination of Hsp70 and Hsp40 (*9*), and the extracellular chaperone clusterin (apolipoprotein J) has been shown to inhibit fibril formation of a number of polypeptides, including Aβ (*10*) and a fragment of the prion protein (*11*). The role of chaperones in prevention of amyloid diseases has not been established. In addition to molecular chaperones, the effects of chemical and pharmacological chaperones have been

[†] This work was supported by the Swedish Research Council (Grant 10371) and FORMAS.

* To whom correspondence should be addressed. Department of Anatomy, Physiology and Biochemistry, The Biomedical Centre, Box 575, 751 23 Uppsala, Sweden. E-mail: jan.johansson@afb.slu.se. Phone: +46-18-4714065. Fax: +46-18-550762.

[‡] Swedish University of Agricultural Sciences.

[§] Uppsala University.

[1] Abbreviations: Aβ, amyloid β-peptide; CTC, C-terminal domain of prosurfactant protein C; ESI, electrospray ionization; MALDI, matrix-assisted laser desorption ionization; SDS−PAGE, sodium dodecyl sulfate−polyacrylamide gel electrophoresis; SP-C, surfactant protein C; SEC, size-exclusion chromatography; TM, transmembrane.

10.1021/bi900135c CCC: $40.75
Published on Web 03/12/2009

studied in the context of misfolding diseases (see, for example, ref *12*). No effective therapy using chaperones or other means has so far been found for any amyloid disease.

Some proteins use part of their prosequence as a scaffold during folding. The importance of prosequence-assisted folding has been established for several proteins, for example, serine proteases (*13*). We have recently shown that the amyloidogenic human lung surfactant protein C (SP-C), generated from proSP-C, has a C-terminal part (CTC, residues 59−197 of proSP-C) that acts in a chaperone-like manner. The mature SP-C peptide corresponds to residues 24−58 of proSP-C and is flanked by an N-terminal domain important for trafficking and stability of the proprotein in the secretory pathway, and CTC. CTC interacts preferably with misfolded, nonhelical, SP-C, prevents SP-C fibril formation in vitro, and prevents aggregation of proSP-C into amyloid-like inclusions in human embryonic kidney 293 (HEK293) cells (*14, 15*).

Johansson et al. recently showed that CTC interacts with the TM part of proSP-C and also shows high affinity for the amino acids Val, Leu, Ile, and Phe, all of which promote insertion of TM segments into the ER membrane (*16, 17*). CTC is thus able to specifically recognize and interact with nonhelical TM regions and prevent them from misfolding. CTC also inhibited Aβ amyloid formation, suggesting that CTC is the first chaperone found to bridge recognition of unfolded TM segments and amyloid prevention (*17*).

Uncovering the properties of CTC might give important insight into new ways of avoiding protein misfolding. To gain more mechanistic information that shows how CTC affects protein aggregation, we have analyzed how CTC interacts with and prevents fibril formation of Aβ_{1-40}, derived form the TM part of its precursor protein. Moreover, the effect of CTC on medin, a peptide that forms amyloid in the aortic wall (*18*), was studied to test the possible generality of CTC anti-amyloid activity.

MATERIALS AND METHODS

Peptides and Materials. Aβ_{1-40} (DAEFRHDSGYEVHHQKLVFFAEDVGSNKGAIIGLMVGGVV) was purchased from Bachem and stored in a lyophilized state at −70 °C until it was used. To promote monomeric starting solutions, the peptide was dissolved, vortexed, and sonicated at 1 mg/mL in dimethyl sulfoxide (DMSO, Merck, Sweden) before being diluted in working buffer. Full-length medin (medin$_{1-50}$, RLDKQGNFNAWVAGSYGNDQWLQVDLGSSKEVTGIITQGARNFGSVQFVA) was purchased from Keck Biotechnology Resource Laboratory (Yale University, New Haven, CT), and medin$_{31-50}$ was a kind gift from K. Sletten at the Biotechnology Center of Oslo (University of Oslo, Oslo, Norway). Chemicals were purchased from Sigma-Aldrich if not stated otherwise.

CTC Expression and Purification. Human recombinant CTC was expressed and purified as described previously (*14, 16*). Briefly, a fragment covering residues 59−197 of human proSP-C was expressed as a fusion protein with thioredoxin, His$_6$, and S tags in *Escherichia coli*. The bacteria were harvested by centrifugation at 6000*g* for 20 min, incubated with lysozyme and DNase in 20 mM Tris-HCl (pH 8) and 2 mM $MgCl_2$, and further loaded onto a Ni-NTA agarose column. After the sample had been washed with 20 mM Tris (pH 8) and with 20 mM Tris (pH 8) containing 20 mM imidazole, target protein was eluted with 150 mM imidazole in 20 mM Tris (pH 8). After dialysis against 20 mM Tris (pH 8), thioredoxin and His tags were cleaved off with thrombin and removed by Ni-NTA agarose chromatography. The protein purity and molecular mass were checked via SDS−PAGE, nondenaturing PAGE, and matrix-assisted laser desorption ionization (MALDI) mass spectrometry. CTC was found to be >95% pure and to have the expected mass. Stock solutions with concentrations of 0.7−1 mM CTC were used for the experiments.

Aβ_{1-40} Aggregation and Fibril Formation. Experiments were conducted with an Aβ concentration of 25 μM in 10 mM sodium phosphate buffer (pH 7.0) and 150 mM sodium chloride containing 10% (v/v) DMSO. Aβ_{1-40} was incubated with and without 2.5 μM CTC at 37 °C under agitation. At various time points, samples were removed to determine the level of aggregation. The samples were centrifuged for 6 min at 16000*g*, and the supernatants were removed and centrifuged for an additional 2 min at 16000*g*. The supernatant from the last centrifugation was then analyzed by SDS−PAGE on 10 to 16% Tris-Tricine gels under nonreducing conditions and stained with Coomassie. As controls, Aβ_{1-40} was incubated with 2.5 μM chicken cystatin (M_w = 13.3 kDa) or human antithrombin (M_w = 58 kDa) in the same manner as described above.

To determine the extent of fibril formation, Aβ_{1-40} was incubated as described above with or without 25 or 2.5 μM CTC, as well as with 25 μM chicken cystatin or bovine serum albumin. After 6 days, the samples were removed and analyzed by transmission electron microscopy (TEM) (see below).

To investigate the ability of CTC to dissociate already formed fibrils, 25 μM Aβ_{1-40} was incubated for 6 days at 37 °C with shaking, the presence of fibrils was verified by TEM, and thereafter, CTC was added to a final concentration of 25 μM. The samples were incubated further for 1−7 days, and thereafter, the amount of fibrils was again estimated using TEM.

Thioflavin T binding was assessed on Aβ_{1-40} (25 μM) incubated in the presence or absence of CTC (25, 12.5, or 2.5 μM) in 10 mM sodium phosphate buffer (pH 7) and 150 mM sodium chloride containing 10% (v/v) DMSO at 37 °C under agitation. At various time points, 10 μL aliquots were removed and diluted to 100 μL with 10 μM thioflavin T (Aldrich) in 10 mM sodium phosphate buffer (pH 7) and 150 mM sodium chloride. The samples were incubated for 5 min in the dark before fluorescence was measured in a FarCyte fluorescence plate reader (GE Healthcare). The wavelengths for excitation and emission were 440 and 480 nm, respectively. Each sample was measured in duplicate.

Medin Aggregation and Fibril Formation. To ensure monomeric starting solutions, both full-length medin (residues 1−50) and a C-terminal part covering residues 31−50 of medin were dissolved in DMSO to final concentrations of 2.5 and 5 mM, respectively. Both full-length medin and the C-terminal fraction were incubated with and without CTC at 1:1 molar ratios in 10 mM phosphate buffer (pH 7.0) and 50 mM sodium chloride with 10% (v/v) DMSO at 20 °C. Medin$_{1-50}$ was incubated at a concentration of 250 μM, and medin$_{31-50}$ was incubated at 500 μM to achieve optimal conditions for fibril formation (*19*). At various time points,

aliquots were removed and fibril formation was assessed using TEM.

Transmission Electron Microscopy (TEM). For each sample, aliquots of 2 μL were adsorbed for 1 min on 200-mesh copper grids and stained with 2% uranyl acetate for 30 s before being examined and photographed using a Hitachi H7100 microscope operated at 75 kV.

Interaction Studies of CTC and Aβ_{1-40} Using Size-Exclusion Chromatography (SEC) and Immunoblot Analysis. SEC was performed using a Superdex 200 column (Amersham Biosciences, Uppsala, Sweden) attached to an FPLC instrument (Amersham Biosciences). The column was equilibrated with 10 mM sodium phosphate buffer (pH 7.0) and 150 mM sodium chloride, and the absorbance at 214 nm was recorded. The column was initially calibrated with fibrinogen (340 kDa), aldolase (158 kDa), bovine serum albumin (67 kDa), and chicken cystatin (13.3 kDa). For the interaction study, three different samples [(i) 34 μM Aβ_{1-40}, (ii) 34 μM CTC, and (iii) 34 μM Aβ_{1-40} and 34 μM CTC] were prepared in 10 mM sodium phosphate buffer (pH 7.0), 150 mM sodium chloride, and 10% (v/v) DMSO. All samples were applied to the column directly after preparation and eluted at a flow rate of 0.7 mL/min using the same buffer that was used for equilibration. Fractions of 1.2 mL were collected from all runs, and 100 μL per fraction was blotted on nitrocellulose membranes (Whatman) using a PR 648 Slot Blot filtration manifold (Amersham Biosciences). For samples containing both Aβ_{1-40} and CTC, two sets of blots were analyzed, to allow detection of both peptides. For detection of Aβ_{1-40}, the membranes were boiled in phosphate-buffered saline (PBS) (pH 7.4) for 5 min and allowed to cool in TBS-Tween (0.1%) before being blocked with 5% nonfat dry milk. The membranes were probed with monoclonal antibody 4G8 (1:2000, Signet) followed by anti-mouse HRP-conjugated secondary antibody (1:5000, GE Healthcare). For detection of S-tagged CTC, the membranes were blocked with 5% nonfat milk and probed with HRP-conjugated S-protein (1:5000, Novagen). Enhanced chemiluminescence (Millipore) was used to detect antibody binding in both cases. Image J (http://rsb.info.nih.gov/ij) was used to measure the intensity of the spots.

MALDI Mass Spectrometry. Aβ_{1-40} was dissolved in DMSO to a concentration of 231 μM and diluted to a concentration of 25 μM with or without 25 μM CTC in 50 mM ammonium acetate buffer (pH 7.0). A sample from each mixture was immediately taken for MALDI analysis. The solutions were then incubated at 37 °C for 2 days with agitation and thereafter for an additional 4 days at 22 °C without shaking. For MALDI analysis, the samples were diluted in 30% acetonitrile with 0.1% trifluoroacetic acid (TFA) to an Aβ_{1-40} concentration of 4 μM, and 0.5 μL of each sample was mixed with 0.5 μL of a 0.8 μM somatostatin solution in 30% acetonitrile and 0.1% TFA. The mixture was applied on top of a layer of sinapinic acid precrystallized on the MALDI target plate from a 20 mg/mL solution in acetone and cocrystallized with 1 μL of sinapinic acid (20 mg/mL) dissolved in 50% acetonitrile and 0.1% TFA. Data between 2000 and 10000 mass to charge ratios (*m*/*z*) were acquired on a Bruker Autoflex apparatus (Bruker Daltonics, Billerica, MA) operated in linear mode employing delayed extraction. One thousand shots were automatically acquired for each sample; for 50 different locations, batches of 20 laser shots per position were averaged using a predefined shooting pattern.

Electrospray Ionization (ESI) Mass Spectrometry. CTC (theoretical average molecular mass of 18264.89 Da) stored at a concentration of 1.1 mM at −20 °C in 20 mM sodium phosphate buffer (pH 7.0) and 30 mM sodium chloride was diluted to 11 μM in ammonium acetate buffer (pH 6.9) for analysis. Aβ_{1-40} (theoretical average molecular mass of 4329.9 Da) was dissolved in 10 mM ammonium bicarbonate buffer (pH 10.8) with 1% (v/v) ammonia, to an Aβ concentration of 100 μM and stored at −20 °C prior to use. When CTC and Aβ_{1-40} were analyzed together, a mixture of 11 μM CTC and 45 μM Aβ_{1-40} was prepared in 10 mM ammonium bicarbonate buffer with a final pH of 7−8. Data were acquired on a QTOF Ultima API mass spectrometer (Waters, Milford, MA) equipped with a Z-spray source, operated in the positive ion mode under the control of MassLynx 4.1, between *m*/*z* 1000 and 5000 with 2 s per scan and an interscan interval of 0.1 s. Samples were introduced via a nanoflow electrospray interface from metal-coated borosilicate glass capillary needles (Proxeon Biosystems, Odense, Denmark), and the source temperature was set to 80 °C. Spraying conditions were tuned with a capillary voltage between 1.2 and 1.9 kV, and cone and RF lens energies were 100 and 38 V, respectively. The pumping of the ES interface region was restricted, increasing the reading on the backing pirani vacuum gauge from 1.8 to 1.95 mbar and employing an analyzer pressure of 5.85×10^{-5} mbar with the use of argon as the collision gas. In MS mode, the collision voltage was set to 10 V, and in MS/MS mode, CTC−Aβ_{1-40} complexes were disrupted by increasing the collision voltage to 80 V. The instrument was operated in V-mode (single-reflector mode) at a resolution of 10000 (full width at half-maximum definition), and the mass scale was calibrated against PEG-3400.

Chaperone Assays. Heat-induced aggregation of alcohol dehydrogenase (ADH) from baker's yeast with and without CTC present was followed at 50 °C for 15 min by measuring the light scattering (apparent absorption at 360 nm) in a Cary 3 spectrophotometer (Varian Techtron, Mulgrave, Australia). All experiments were conducted with ADH and CTC concentrations of 6.25 μM each, and the samples were prepared in 20 mM sodium phosphate buffer (pH 7.4) and 150 mM sodium chloride. Reduction-induced aggregation of the β-chain of insulin with and without CTC was likewise monitored by measuring the apparent absorption at 360 nm. A solution containing 40 μM insulin (Sigma) in 50 mM sodium phosphate buffer (pH 7.0) and 100 mM sodium chloride, with or without CTC, at a molar ratio of 1:1 was preincubated for 5 min at 41 °C. Dithiothreitol (DTT) was then added to a final concentration of 20 μM, and the change in absorption at 360 nm was monitored for 15 min at 41 °C.

RESULTS

CTC Prevents Aβ_{1-40} Aggregation and Fibril Formation. Aβ_{1-40} was incubated in the presence and absence of CTC at 1:1 and 10:1 molar ratios. TEM images obtained after incubation for 6 days showed that fibril formation of Aβ_{1-40} was completely abolished in the presence of CTC even at less than equimolar ratios (Figure 1). Neither chicken cystatin

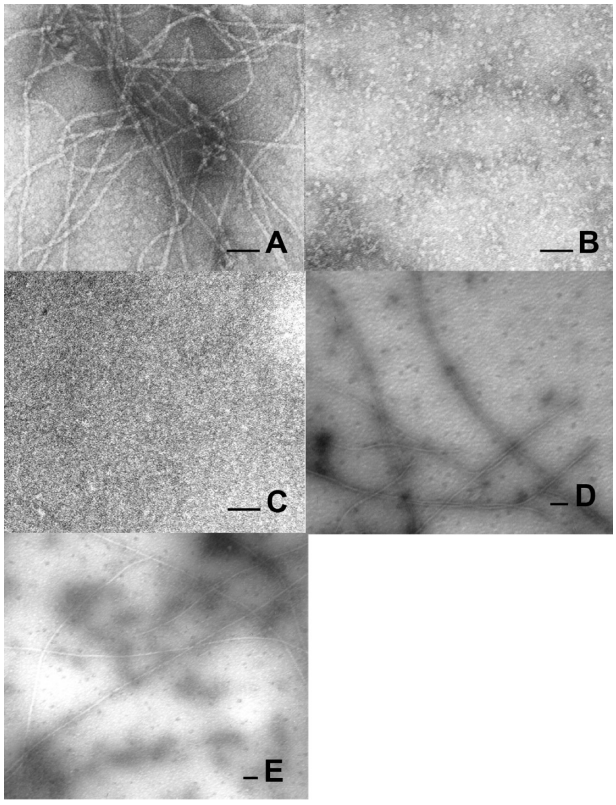

FIGURE 1: CTC prevents Aβ_{1-40} fibril formation. Transmission electron micrographs of 25 μM Aβ_{1-40} incubated at 37 °C in 10 mM sodium phosphate buffer (pH 7.0) and 150 mM sodium chloride with 10% DMSO (v/v) for 6 days alone (A), together with 25 μM CTC (B), together with 2.5 μM CTC (C), together with 25 μM BSA (D), or together with 25 μM chicken cystatin (E). The scale bar is 100 nm.

nor BSA in equimolar amounts relative to Aβ_{1-40} prevented Aβ_{1-40} fibril formation (Figure 1), indicating the specificity of the interaction between CTC and Aβ_{1-40}.

Preformed amyloid fibrils of Aβ_{1-40} were incubated with CTC at a 1:1 molar ratio relative to the Aβ_{1-40} concentration used to form the fibrils. No change in the amount or appearance of fibrils observed by TEM was seen after incubation with CTC for up to 7 days (data not shown). These experiments indicate that CTC does not have the ability to dissociate already formed fibrils but rather interacts with species on the pathway to fibril formation.

Thioflavin T binding experiments showed that CTC reduces the level of Aβ_{1-40} polymerization at 1:1, 1:2, and 1:10 molar ratios (Figure 2). While CTC at an equimolar or 1:2 molar ratio completely prevents Aβ_{1-40} polymerization, 10 times less CTC than Aβ_{1-40} results in prolongation of the lag phase only.

SDS−PAGE was utilized to further study the effects of CTC on Aβ aggregation. Aβ_{1-40} was incubated with CTC as well as the control protein chicken cystatin or human antithrombin at Aβ:protein molar ratios of 10:1. The amounts of Aβ at time zero were equal for all mixtures, but after 7 days, no Aβ was seen from the sample with Aβ alone or the sample co-incubated with chicken cystatin. Minute amounts of soluble Aβ were seen in the sample co-incubated with antithrombin, while the sample containing CTC showed almost equal amounts of soluble Aβ as seen at time zero (Figure 3A). Even after co-incubation of CTC and Aβ for 20 days, soluble Aβ was found (Figure 3B).

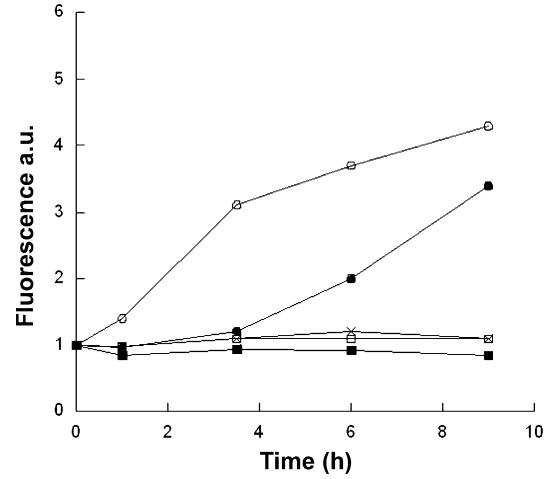

FIGURE 2: CTC inhibits Aβ_{1-40} polymerization. Thioflavin T fluorescence after different periods of incubation of 25 μM Aβ_{1-40} alone in 10 mM phosphate buffer (pH 7.0) and 150 mM sodium chloride with 10% DMSO (○) or in the presence of 25 (□), 12.5 (×), or 2.5 μM CTC (●). A sample of 25 μM CTC alone (■) was also included. Samples were measured in duplicate and showed a variability of <10%.

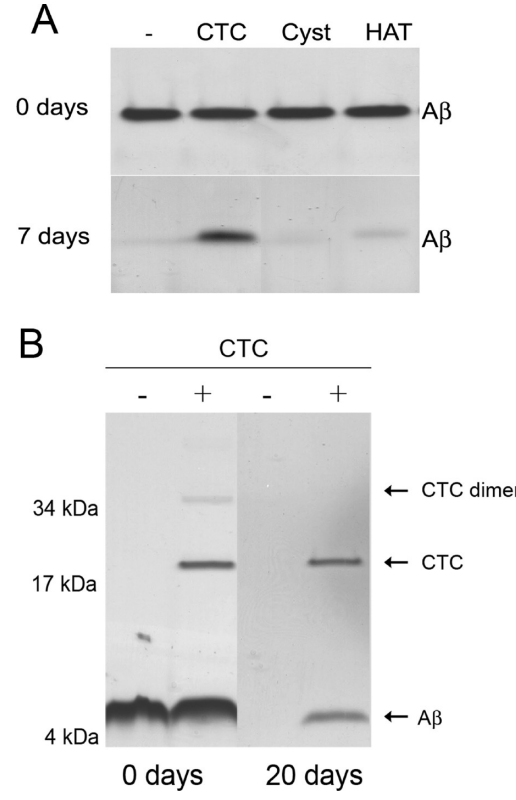

FIGURE 3: CTC prevents aggregation of Aβ_{1-40}. SDS−PAGE of 16000*g* soluble fractions of (A) 25 μM Aβ_{1-40} incubated for 0 and 7 days in the presence or absence of 2.5 μM CTC, chicken cystatin (Cyst), or human antithrombin (HAT) and (B) 25 μM Aβ_{1-40} incubated for 0 or 20 days in the presence or absence of 2.5 μM CTC. All incubations were performed in 10 mM sodium phosphate buffer (pH 7.0) and 150 mM sodium chloride with 10% (v/v) DMSO.

An inhibitory effect on Aβ_{1-40} aggregation by CTC was also evident with MALDI-MS. Aβ_{1-40} incubated with or without equimolar amounts of CTC was analyzed for the presence of monomeric and soluble Aβ. MALDI-MS gives reliable concentration estimates for peptides when using internal standards (*20*). In our experiments, we used soma-

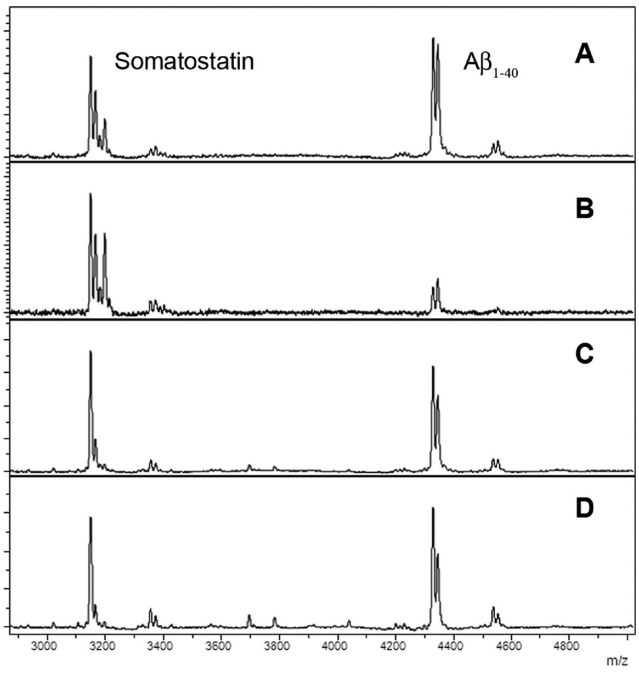

FIGURE 4: CTC keeps $A\beta_{1-40}$ in a soluble, monomeric state. Quantification of $A\beta_{1-40}$ (theoretical mass of 4329.86 Da) in solution assessed by MALDI-MS using somatostatin (theoretical mass of 3149.61 Da) as an internal standard. Panels A and B show 25 μM $A\beta_{1-40}$ incubated alone, and panels C and D show 25 μM $A\beta_{1-40}$ incubated together with 25 μM CTC. Samples used for panels A and C were analyzed before incubation, and samples used for panels B and D were analyzed after incubation for 2 days at 37 °C with agitation and for an additional 4 days at 22 °C in 50 mM ammonium acetate buffer (pH 7.0).

tostatin, a known nonaggregating peptide, as an internal standard and employed automatic collection from several different points for each MALDI target to minimize human errors and biases. Using this method, a good correlation between somatostatin and $A\beta_{1-40}$ concentrations was obtained ($R^2 > 0.9$). $A\beta_{1-40}$ incubated alone exhibited a 80% decrease in soluble peptide relative to somatostatin (Figure 4A,B), whereas in the samples containing both $A\beta_{1-40}$ and CTC, the amount of soluble $A\beta_{1-40}$ remained constant over the time period analyzed (Figure 4C,D).

CTC and $A\beta_{1-40}$ Form Complexes. SEC coupled with immunoblotting was employed to study the interaction between $A\beta_{1-40}$ and CTC. The 214 nm absorbance profile for $A\beta_{1-40}$ showed a pattern compatible with the presence of low-number oligomeric species and a small amount of larger species eluting in the void volume (not shown), indicating the presence of prefibrillar soluble oligomers. In the $A\beta_{1-40}$−CTC sample, the larger $A\beta$ species were absent, which further supports the results from the aggregation assays. CTC on its own appeared as two groups of oligomers. The clearly dominating peak eluted at a position corresponding to the size of trimers to pentamers, and another peak eluted at a position corresponding to dodecamers. This result is in good agreement with analytical ultracentrifugation and ESI mass spectrometry data showing that CTC trimers and oligomers thereof are the main species (*21*).

The SEC profile for the $A\beta_{1-40}$−CTC sample showed that the magnitude of the peak corresponding to CTC trimers to pentamers increased ~30% compared to that for the elution of CTC alone, which suggests that $A\beta$ binds to and stabilizes CTC trimers to pentamers. No unique peak corresponding to an $A\beta$−CTC complex could be detected by absorbance measurements, possibly due to the comparatively large elution volume of CTC alone. SEC of a mixture of $A\beta_{1-40}$ and CTC followed by dot blot analysis of fractions, however, clearly showed a unique peak compared to the polypeptides alone (Figure 5). This indicates that $A\beta$ and CTC interact and form a stable complex. The new peak observed corresponds to a complex of ~110 kDa and was accompanied by a loss of the $A\beta$ peak corresponding to ~52 kDa (Figure 5B,C). Suggestively, the new species could thus be a 12-mer of $A\beta_{1-40}$ (52 kDa) bound to a trimer of CTC (55 kDa), but alternative compositions cannot be excluded.

To further study formation of the $A\beta$−CTC complex, the mixture of $A\beta_{1-40}$ and CTC as well as the separate polypeptides was analyzed using ESI mass spectrometry. Comparison of the peak pattern obtained from the individual peptides and the mixed sample indicated formation of complexes between $A\beta_{1-40}$ and CTC. CTC oligomers were found (Figures 6 and 7A, peaks not annotated), in agreement with previous observations (*21*). For the mixture, several peaks not corresponding to homomers of CTC or $A\beta$ but which could instead be assigned to CTC−$A\beta$ heteromers appeared (Figure 6). Peaks of low intensity corresponding to one CTC bound to one $A\beta_{1-40}$ with nine (*m*/*z* 2511) or ten (*m*/*z* 2260) charges were found. A complete charge state envelope with 16−23 charges (*m*/*z* 3696−2572) corresponding to a trimer of CTC in complex with one $A\beta_{1-40}$ peptide was seen.

The peak at *m*/*z* 3485 (Figure 6), not found in the spectrum of CTC alone, corresponding to $[3CTC+A\beta]^{17+}$ was selected for MS/MS to verify that it represents a complex of the two peptides (Figure 7B). The collision voltage was increased from 10 to 80 V which apparently was enough to disrupt part of the complex. This yielded a number of daughter ions, mainly corresponding to monomers of CTC and $A\beta_{1-40}$, but also to CTC trimers (Figure 7C,D). Interestingly, among the daughter ions were found hexamers of CTC, indicating that at least a portion of the selected ions in fact corresponds to $[6CTC+2A\beta]^{34+}$ or larger heteromers. Also present in the spectrum after collision was a heteromer consisting of dimeric CTC and monomeric $A\beta_{1-40}$ with ten (*m*/*z* 4087) and nine (*m*/*z* 4541) charges, which was not found in MS mode (data not shown).

CTC Lacks Classical Chaperone Activity. To asses the ability of CTC to act as a classical chaperone, i.e., to prevent aggregation of destabilized proteins, assays employing either ADH or insulin were used. At 50 °C, ADH started to aggregate within 5 min. Addition of CTC in equimolar amounts resulted in a minor prolongation of the lag phase before ADH started to aggregate (Figure 8A). This effect is small compared to the effects of a chaperone like, for example, the sHsp α-crystallin which results in complete prevention of ADH aggregation (*22*). Reduction of insulin at 41 °C resulted in aggregation after ~3 min (Figure 8B). Addition of CTC at a molar ratio of 1:1 did not affect insulin aggregation at all (Figure 8B). It appears from these results that CTC does not act in a manner typical for traditional chaperones.

CTC Prevents Medin Fibril Formation. Medin was incubated with and without CTC to see if the effects observed for CTC on SP-C and $A\beta_{1-40}$ fibril formation could be applicable to yet another amyloidogenic peptide. Both the 50-residue full-length medin and the C-terminal part, residues

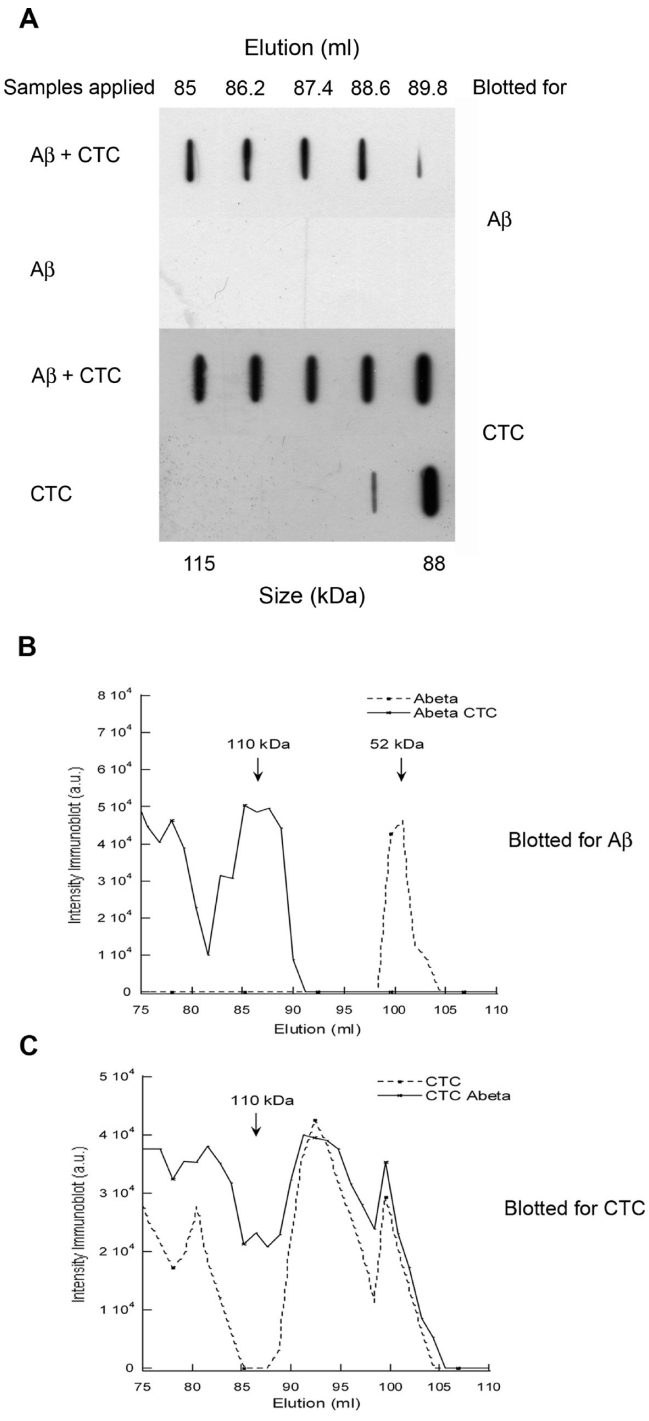

FIGURE 5: CTC and Aβ_{1-40} complexes analyzed by SEC. (A) Immunoblot analyses of SEC fractions corresponding to elution volumes of 85−89 mL. The polypeptide contents in the samples applied to the column are indicated at the left. The top two rows were probed with antibody 4G8, recognizing Aβ_{1-40}, and the two bottom rows were probed with an HRP-conjugated S-protein for detection of CTC. (B and C) Intensities of immunoblots of SEC fractions corresponding to elution volumes of 75−110 mL. The blots were probed with either antibody 4G8 (B) or S-protein (C). Data for blots from samples containing Aβ and CTC are represented by solid lines, while data for blots from samples of Aβ alone (B) and CTC alone (C) are represented by dotted lines. The arrows mark molecular masses estimated from elution positions of proteins with known masses. The figure is representative of three independent runs.

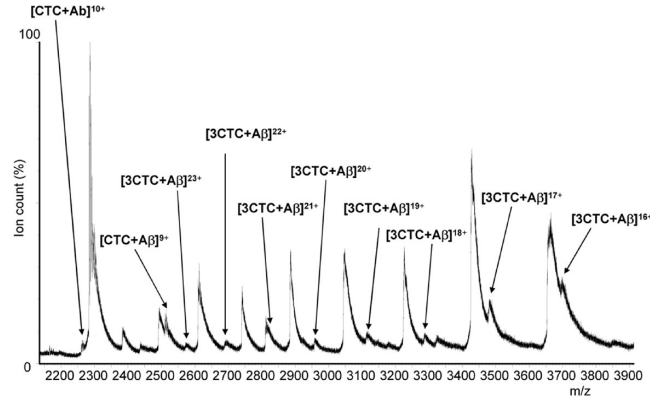

FIGURE 6: CTC interacts with and forms complexes with Aβ_{1-40}. Nanospray ESI-MS spectrum of 11 μM CTC mixed with 45 μM Aβ_{1-40}. Labeled peaks correspond to complexes formed between CTC and Aβ_{1-40} with different charge states, as deduced from spectra of CTC or Aβ_{1-40} alone (see also Figure 7).

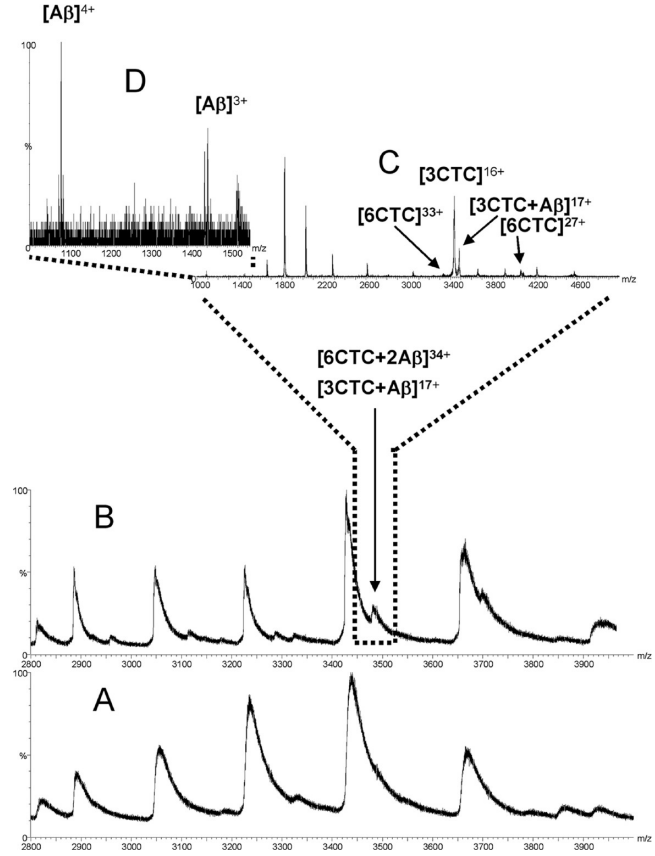

FIGURE 7: Analysis of the CTC−Aβ complex by MS/MS. Nanospray ESI-MS spectrum of (A) CTC and (B) CTC mixed with Aβ_{1-40}. (C) MS/MS spectra of the ion observed at *m/z* 3484 in the mixed sample in panel B. The collision voltage was 80 V. (D) Enlargement of the *m/z* range between 1000 and 1600 from panel C, with peaks corresponding to Aβ_{1-40} released from the CTC−Aβ complex labeled.

31−50, which is more prone to forming fibrils (*19*), were studied. After incubation for 4 days, medin$_{31-50}$ showed large amounts of amyloid fibrils as judged by the TEM images (Figure 9A). Addition of CTC at a 1:1 molar ratio completely abolished the formation of fibrils (Figure 9B). Full-length medin after 14−21 days formed amyloid fibrils that appeared to be longer than the ones seen with medin$_{31-50}$. Fibril formation of medin$_{1-50}$ was likewise prevented by the presence of CTC (Figure 9C,D). These results further strengthen the emerging picture that CTC can recognize and bind peptide species on the pathway to amyloid fibrils and prevent them from polymerizing.

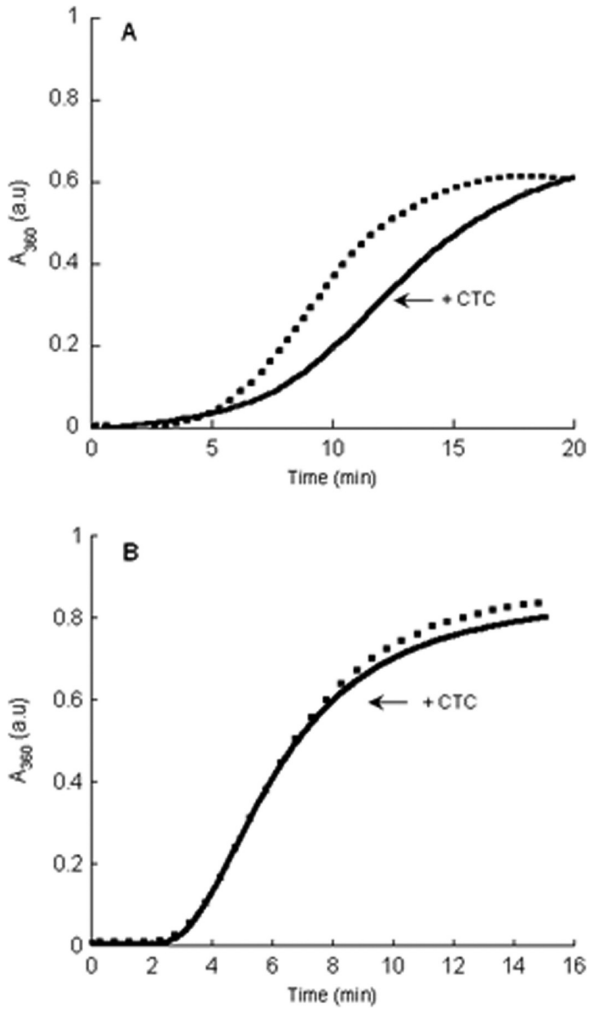

FIGURE 8: CTC lacks classical chaperone activity. (A) Heat-induced aggregation of ADH observed by light scattering in the absence (•••) and presence (—) of equimolar amounts of CTC. (B) Reduction-induced aggregation of insulin observed by light scattering in the absence (•••) and presence (—) of equimolar amounts of CTC.

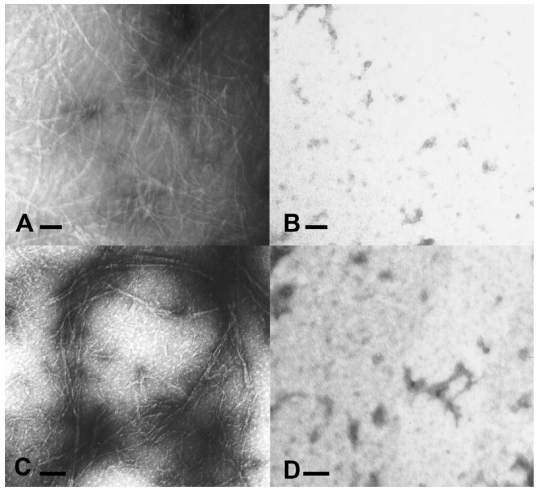

FIGURE 9: CTC inhibits fibril formation of medin. Transmission electron micrographs of fibrils formed from (A) 500 μM $medin_{31-50}$ incubated alone, (B) 500 μM $medin_{31-50}$ incubated with 500 μM CTC, (C) 250 μM $medin_{1-50}$ incubated alone, or (D) 250 μM $medin_{1-50}$ incubated with 250 μM CTC. All incubations were performed at 20 °C in 10 mM phosphate buffer (pH 7.0), 50 mM sodium chloride, with 10% (v/v) DMSO. The scale bar is 100 nm.

DISCUSSION

Protein misfolding and aggregation into amyloid fibrils are associated with a number of severe diseases for which there are no cure. These so-called misfolding diseases include, for example, Alzheimer's disease, Parkinson's disease, and Creutzfelt-Jacobs disease. Finding therapeutic strategies to prevent or treat these disorders is an important and challenging task. Molecular chaperones may be one possible therapeutic strategy for interfering with the aggregation process. In this study, we have investigated the newly discovered chaperone CTC and its effect on amyloid fibril formation.

The molecular chaperones Hsp70 and Hsp90, which colocalize with plaques associated with Alzheimer's disease (*23, 24*), are able to inhibit the aggregation of Aβ at an early stage but are unable to exert any effect on already formed fibrils (*9*). However, it has been shown that Hsp104 can dissociate already formed fibrils of Sup35 (*25*).

Small heat shock proteins (sHSPs) make up a family of intracellular molecular chaperones that colocalize with a number of disease-associated protein aggregates such as senile plaques in Alzheimer's disease and Lewy bodies in Parkinson's disease. These chaperones have a mass of <40 kDa and a highly conserved C-terminal sequence of ~100 residues called the α-crystallin domain (*26*). Hydrophobic sites are believed to be responsible for the chaperone activity of the sHSPs. Interestingly, the hydrophobic peptide region of residues 70−88, which is part of the α-crystallin domain of αA-crystallin, has been shown to be able to inhibit Aβ fibril formation (*27*).

Apolipoprotein J, alias clusterin, is an extracellular protein that is able to inhibit amorphous aggregation of a variety of proteins (*28*) by interacting with exposed hydrophobic patches, like small heat shock proteins. Yerbury et al. (*29*) have shown that clusterin is also able to inhibit fibril formation, by forming stable complexes, with a number of amyloidogenic proteins such as Aβ, α-synuclein, and lysozyme, and it was suggested that clusterin recognizes and interacts with structural features common to prefibrillar species.

proSP-C is a TM protein expressed in epithelial type II cells and has a discordant helix, making up the TM region (*7*). The (pro)SP-C helix can misfold and form amyloid fibrils associated with disease. CTC contains a domain of ~100 amino acids known as a Brichos domain. Brichos domains are found in several other proteins associated with proliferative and degenerative disease, for example, Bri associated with British dementia, and one of its initially suggested functions was a chaperone-like role (*30*), which has been experimentally supported for the proSP-C Brichos domain (*14*−*17*). It has also been shown that CTC and its Brichos domain interact with stretches of nonpolar residues. The substrate specificity of CTC thus coincides with residues that promote TM insertion (*17*). These findings led us to study whether the chaperone activity of CTC extends to other amyloidogenic peptides.

Herein, we show that recombinant human CTC can prevent amyloid formation of the Alzheimer's disease-associated peptide $A\beta_{1-40}$, an amyloidogenic peptide which resembles SP-C in that it contains a discordant helix (residues 16−23) and originates from the TM domain of the APP (ap-

proximately residues 29−40). CTC potently inhibits fibril formation even at substochiometric ratios (Figures 1and 2) but is not able to dissociate preformed fibrils, suggesting that it interacts with early species on the amyloid pathway. As seen in Figure 3, CTC is able to keep Aβ in a soluble state for up to 20 days, and the inability of control proteins similar in size to do so further indicates that the CTC effect is based on specific interactions. MALDI mass spectrometry was also used to study the effect of CTC, which showed that CTC has an inhibitory effect on aggregation of Aβ_{1-40}. Thioflavin T experiments also showed that CTC is able to block aggregation of Aβ_{1-40}. Using 10 times less CTC than Aβ_{1-40} resulted in formation of ThT-positive species after a prolonged lag phase. Since a 1:10 CTC:Aβ_{1-40} ratio results in no detectable fibrils and keeps Aβ in a soluble state, it is possible that the ThT-positive species represent nonfibrillogenic and soluble aggregates.

To study the mechanism of interaction and determine the stoichiometry of the CTC−Aβ complexes, SEC and ESI mass spectrometry were employed. SEC showed that the two molecules interact and form complexes that are stable during chromatography. It appears that the complexes formed are composed of a CTC trimer interacting with an Aβ 12-mer. Interestingly, an oligomer denoted Aβ*56 (a 56 kDa species supposedly composed of 12 Aβ molecules) was isolated by SDS−PAGE and found to confer memory loss in rodents (*31*). These findings are compatible with the existence of Aβ oligomers, possibly micellar-like structures (*32*) that are able to stay intact during SEC and SDS−PAGE and to associate with CTC. Using ESI mass spectrometry, the main complex found was that of a CTC trimer interacting with monomeric Aβ (Figure 6). CID experiments confirmed the Aβ−CTC nature of the complex (Figure 7). The stoichiometries of the CTC−Aβ complexes apparently differ between SEC and ESI-MS data. SEC data on aggregation-prone peptides must be analyzed with care as it is possible that large aggregates would be retained on the SEC column or elute in the void volume. However, it is not likely that the CTC trimer−Aβ complex seen using ESI-MS would be lost in the SEC experiment. Also, ESI-MS might be more efficient than SEC in breaking up Aβ micelles or similar aggregates, without disrupting direct CTC−Aβ interactions. Combining the SEC and ESI-MS data suggests that a CTC trimer can bind to one Aβ molecule present in an approximately dodecameric assembly.

With the aim of investigating whether the anti-amyloid function of CTC could be applicable to yet another polypeptide, the effects on fibril formation of medin were studied. Medin, which is a 50-amino acid residue peptide derived from the glycoprotein lactadherin, is associated with aortic amyloidosis in virtually all individuals who are more than 50 years of age. Upon cleavage, normally embedded β-strands are exposed which enables amyloid formation (*18*). CTC inhibits medin fibril formation, further strengthening the idea of CTC as chaperone with specific anti-amyloid properties (Figure 9).

CTC has been shown to recognize five- to seven-residue peptide segments that contain mainly Val, Ile, Leu, Phe, or Tyr and are in a nonhelical conformation. This substrate specificity is similar to that of chaperones such as the ER-localized BiP and the cytosolic Hsp70 analogue DnaK but shows distinct differences (*17*). CTC is unable to prevent aggregation of ADH and insulin (Figure 8). This further indicates that it does not possess the same binding properties as chaperones such as Hsp70 and sHsps.

The amino acids recognized by CTC are associated with membrane insertion according to the "biological" hydrophobicity scale (*33*), which suggests that CTC can interact with TM regions in general. Some amyloidogenic proteins have TM regions associated with their aggregation, e.g., one topologic variant of the prion protein (*34*) and Aβ (*4*). It is also notable that proteins associated with membranes via amphipathic helices, e.g., apolipoproteins, are frequent among amyloidogenic proteins (*35*). The amyloid-promoting domain in medin has been mapped to the C-terminal part using TANGO analysis and various aggregation assays (*19*). The medin C-terminal part has a high degree of Ile, Val, and Phe (e.g., F_{43}GSYGFY_{49}) which is consistent with the CTC substrate specificity. Chiti et al. (*36*) investigated which parameters affect protein aggregation rates and found that high β-sheet/low α-helix secondary structure propensity, hydrophobicity, and low overall charge are main determinants for amyloid formation. Some properties associated with amyloidogenic behavior are thus reminiscent of key features of membrane proteins, in particular their TM segments. This may explain the dual function of CTC to chaperone misfolded TM segments and prevent amyloid formation.

Here we have studied the effect of CTC on amyloid fibril formation of Aβ_{1-40} and medin. CTC is expressed in alveolar type II cells, and whether it is retained intracellularly or secreted, like mature SP-C, is not known. The different tissue distributions of CTC and amyloid-forming peptides studied herein likely preclude interactions in vivo. However, the mechanism by which CTC acts on amyloidogenic proteins and prevents their aggregation could give important insights into anti-amyloid strategies and be used in development of compounds that prevent peptide aggregation.

In conclusion, a general anti-amyloid activity for CTC, a protein domain previously shown to interact with nonhelical TM segments and prevent amyloid fibril formation during proSP-C biosynthesis, has been investigated. We propose that CTC is the first known chaperone directed against unfolded TM segments with an ability to recognize amyloidogenic polypeptides and prevent their aggregation. These properties could make it a useful diagnostic or therapeutic agent, possibilities that require further testing.

ACKNOWLEDGMENT

We are grateful to J. Sjövall, G. Alvelius, and J. Lengqvist for discussions concerning mass spectrometry and to P. Westermark for helpful comments on the manuscript.

REFERENCES

1. Westermark, P., Benson, M. D., Buxbaum, J. N., Cohen, A. S., Frangione, B., Ikeda, S., Masters, C. L., Merlini, G., Saraiva, M. J., and Sipe, J. D. (2005) Amyloid: Toward terminology clarification. Report from the Nomenclature Committee of the International Society of Amyloidosis. *Amyloid 12*, 1–4.
2. Serpell, L. C. (2000) Alzheimer's amyloid fibrils: Structure and assembly. *Biochim. Biophys. Acta 1502*, 16–30.
3. Stefani, M., and Dobson, C. M. (2003) Protein aggregation and aggregate toxicity: New insights into protein folding, misfolding diseases and biological evolution. *J. Mol. Med. 81*, 678–699.
4. Hardy, J., and Selkoe, D. J. (2002) The amyloid hypothesis of Alzheimer's disease: Progress and problems on the road to therapeutics. *Science 297*, 353–356.

5. Bucciantini, M., Calloni, G., Chiti, F., Formigli, L., Nosi, D., Dobson, C. M., and Stefani, M. (2004) Prefibrillar amyloid protein aggregates share common features of cytotoxicity. *J. Biol. Chem. 279*, 31374–31382.
6. Haass, C. (2004) Take five: BACE and the γ-secretase quartet conduct Alzheimer's amyloid β-peptide generation. *EMBO J. 23*, 483–488.
7. Kallberg, Y., Gustafsson, M., Persson, B., Thyberg, J., and Johansson, J. (2001) Prediction of amyloid fibril-forming proteins. *J. Biol. Chem. 276*, 12945–12950.
8. Hardy, J. A., and Higgins, G. A. (1992) Alzheimer's disease: The amyloid cascade hypothesis. *Science 256*, 184–185.
9. Evans, C. G., Wisen, S., and Gestwicki, J. E. (2006) Heat shock proteins 70 and 90 inhibit early stages of amyloid β-(1−42) aggregation in vitro. *J. Biol. Chem. 281*, 33182–33191.
10. Matsubara, E., Soto, C., Governale, S., Frangione, B., and Ghiso, J. (1996) Apolipoprotein J and Alzheimer's amyloid β solubility. *Biochem. J. 316* (Part 2), 671–679.
11. McHattie, S., and Edington, N. (1999) Clusterin prevents aggregation of neuropeptide 106−126 in vitro. *Biochem. Biophys. Res. Commun. 259*, 336–340.
12. Chaudhuri, T. K., and Paul, S. (2006) Protein-misfolding diseases and chaperone-based therapeutic approaches. *FEBS J. 273*, 1331–1349.
13. Eder, J., and Fersht, A. R. (1995) Pro-sequence-assisted protein folding. *Mol. Microbiol. 16*, 609–614.
14. Johansson, H., Nordling, K., Weaver, T. E., and Johansson, J. (2006) The Brichos domain-containing C-terminal part of pro-surfactant protein C binds to an unfolded poly-val transmembrane segment. *J. Biol. Chem. 281*, 21032–21039.
15. Nerelius, C., Martin, E., Peng, S., Gustafsson, M., Nordling, K., Weaver, T., and Johansson, J. (2008) Mutations linked to interstitial lung disease can abrogate anti-amyloid function of prosurfactant protein C. *Biochem. J. 416*, 201–209.
16. Johansson, H., Eriksson, M., Nordling, K., Presto, J., and Johansson, J. (2009) The Brichos domain of prosurfactant protein C can hold and fold a transmembrane segment, manuscript submitted for publication. *Protein Sci.* (in press).
17. Johansson, H., Nerelius, C., Nordling, K., and Johansson, J. (2009) Preventing amyloid formation by catching unfolded transmembrane segments. *J. Mol. Biol.* (manuscript submitted for publication).
18. Haggqvist, B., Naslund, J., Sletten, K., Westermark, G. T., Mucchiano, G., Tjernberg, L. O., Nordstedt, C., Engstrom, U., and Westermark, P. (1999) Medin: An integral fragment of aortic smooth muscle cell-produced lactadherin forms the most common human amyloid. *Proc. Natl. Acad. Sci. U.S.A. 96*, 8669–8674.
19. Larsson, A., Soderberg, L., Westermark, G. T., Sletten, K., Engstrom, U., Tjernberg, L. O., Naslund, J., and Westermark, P. (2007) Unwinding fibril formation of medin, the peptide of the most common form of human amyloid. *Biochem. Biophys. Res. Commun. 361*, 822–828.
20. Hosia, W., Johansson, J., and Griffiths, W. J. (2002) Hydrogen/deuterium exchange and aggregation of a polyvaline and a polyleucine α helix investigated by matrix-assisted laser desorption ionization mass spectrometry. *Mol. Cell. Proteomics 1*, 592–597.
21. Casals, C., Johansson, H., Saenz, A., Gustafsson, M., Alfonso, C., Nordling, K., and Johansson, J. (2008) C-Terminal, endoplasmic reticulum-lumenal domain of prosurfactant protein C: Structural features and membrane interactions. *FEBS J. 275*, 536–547.
22. Clark, J. I., and Huang, Q. L. (1996) Modulation of the chaperone-like activity of bovine α-Crystallin. *Proc. Natl. Acad. Sci. U.S.A. 93*, 15185–15189.
23. Hamos, J. E., Oblas, B., Pulaski-Salo, D., Welch, W. J., Bole, D. G., and Drachman, D. A. (1991) Expression of heat shock proteins in Alzheimer's disease. *Neurology 41*, 345–350.
24. Kakimura, J., Kitamura, Y., Takata, K., Umeki, M., Suzuki, S., Shibagaki, K., Taniguchi, T., Nomura, Y., Gebicke-Haerter, P. J., Smith, M. A., Perry, G., and Shimohama, S. (2002) Microglial activation and amyloid-β clearance induced by exogenous heat-shock proteins. *FASEB J. 16*, 601–603.
25. Shorter, J., and Lindquist, S. (2004) Hsp104 catalyzes formation and elimination of self-replicating Sup35 prion conformers. *Science 304*, 1793–1797.
26. Muchowski, P. J., and Wacker, J. L. (2005) Modulation of neurodegeneration by molecular chaperones. *Nat. Rev. Neurosci. 6*, 11–22.
27. Santhoshkumar, P., and Sharma, K. K. (2004) Inhibition of amyloid fibrillogenesis and toxicity by a peptide chaperone. *Mol. Cell. Biochem. 267*, 147–155.
28. Humphreys, D. T., Carver, J. A., Easterbrook-Smith, S. B., and Wilson, M. R. (1999) Clusterin has chaperone-like activity similar to that of small heat shock proteins. *J. Biol. Chem. 274*, 6875–6881.
29. Yerbury, J. J., Poon, S., Meehan, S., Thompson, B., Kumita, J. R., Dobson, C. M., and Wilson, M. R. (2007) The extracellular chaperone clusterin influences amyloid formation and toxicity by interacting with prefibrillar structures. *FASEB J. 21*, 2312–2322.
30. Sanchez-Pulido, L., Devos, D., and Valencia, A. (2002) BRICHOS: A conserved domain in proteins associated with dementia, respiratory distress and cancer. *Trends Biochem. Sci. 27*, 329–332.
31. Lesne, S., Koh, M. T., Kotilinek, L., Kayed, R., Glabe, C. G., Yang, A., Gallagher, M., and Ashe, K. H. (2006) A specific amyloid-β protein assembly in the brain impairs memory. *Nature 440*, 352–357.
32. Barghorn, S., Nimmrich, V., Striebinger, A., Krantz, C., Keller, P., Janson, B., Bahr, M., Schmidt, M., Bitner, R. S., Harlan, J., Barlow, E., Ebert, U., and Hillen, H. (2005) Globular amyloid β-peptide oligomer: A homogenous and stable neuropathological protein in Alzheimer's disease. *J. Neurochem. 95*, 834–847.
33. Hessa, T., Kim, H., Bihlmaier, K., Lundin, C., Boekel, J., Andersson, H., Nilsson, I., White, S. H., and von Heijne, G. (2005) Recognition of transmembrane helices by the endoplasmic reticulum translocon. *Nature 433*, 377–381.
34. Hegde, R. S., Mastrianni, J. A., Scott, M. R., DeFea, K. A., Tremblay, P., Torchia, M., DeArmond, S. J., Prusiner, S. B., and Lingappa, V. R. (1998) A transmembrane form of the prion protein in neurodegenerative disease. *Science 279*, 827–834.
35. Westermark, P. (2005) Aspects on human amyloid forms and their fibril polypeptides. *FEBS J. 272*, 5942–5949.
36. Chiti, F., Stefani, M., Taddei, N., Ramponi, G., and Dobson, C. M. (2003) Rationalization of the effects of mutations on peptide and protein aggregation rates. *Nature 424*, 805–808.

BI900135C